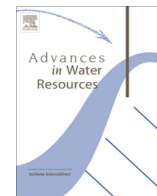




Contents lists available at ScienceDirect

Advances in Water Resources

journal homepage: www.elsevier.com/locate/advwatres

A numerical investigation of mixing and spreading across an angled discontinuity

Brandon Schneider^a, Amir Paster^b, Diogo Bolster^{a,*}

^a Dept. of Civil and Environmental Engineering and Earth Sciences, University of Notre Dame, Notre Dame, IN 46556, USA

^b The Iby and Aladar Fleischman Faculty of Engineering, Tel Aviv University, Ramat Aviv 69978, Israel

ARTICLE INFO

Article history:
Available online xxx

Keywords:
Dilution
Mixing
Spreading
Transverse dispersion

ABSTRACT

We study mixing and spreading in a very simple heterogeneous system: a numerical flow cell comprised of two homogeneous porous media separated by a sharp angled interface. The two media have identical porosity, but differing permeability and dispersivity characteristics representing a fine and a coarse medium. We focus on transport in advection-dominated systems as the primary role of the angled interface is to distort the velocity field. We demonstrate that the angle of the interface influences spreading in the system as observed by depth averaged breakthrough curves, but that the direction of flow does not appear to have a significant role on this. We also study evolution of mixing in the system as quantified by the dilution index. We demonstrate that when transverse dispersion is neglected global rates of mixing appear very similar for all considered interface angles, despite discernible differences in spreading. As a consequence this paper demonstrates that systems with quite different spreading characteristics can have similar mixing characteristics, and likewise systems with identical spreading characteristics can have quite different mixing. This work reinforces the limited applicability of using information from depth averaged breakthrough curves in assessing mixing and mixing driven phenomena.

© 2013 Elsevier Ltd. All rights reserved.

1. Introduction

Mixing is an essential driver of chemical reactions in groundwater; however its quantification in practice is challenging [37,29,91]. In the context of contaminant transport, mixing describes the rate at which reactive species meet, and its accurate representation is becoming increasingly recognized as critical in better understanding various geochemical and biogeochemical processes [5,41,64,78]. Effective in situ remediation for example can depend largely on the interplay between injected masses [27,51,61,75,74,77,89]. In previous works, two common metrics applied to study global mixing include (i) the dilution index [63], a metric related to entropy that describes the overall mixing state of a system, and (ii) the scalar dissipation rate, an integrated form of the local mixing rate [36,46,70].

Complexities inherent in porous media such as heterogeneous permeability are commonly observed in natural systems [33]. These can distort groundwater flow, impacting spreading and mixing rates [39]. The specific relationship between intrinsic heterogeneities and characteristic mixing rates has received some attention, yet macroscopic models that predict reactive transport often still rely on upscaled parameters and are not always capable of capturing observed reaction rates [53,73,85]. Previous modeling work has shown that the amount of mixing depends largely on velocity

fluctuations [82,7,40,70,24,17,35]. Although mixing can be difficult to measure, much research has been devoted to predicting spreading, and many successful models have emerged [31,32,50,79]. A variety of modeling approaches including volume averaging [95], the method of moments [45], homogenization [57] and method of multiple scales [6] have emerged to predict asymptotic dispersion, a measure of spreading. It is also worth noting that pre-asymptotic (non-Fickian) transport characteristics can also be a measure of spreading, especially in highly heterogeneous porous media where asymptotic transport may not be attained. Several alternative theories that aim to capture spreading in these non-Fickian systems also exist (e.g. [12,13,68,69,76]). Most work on spreading has focused on matching the evolution of a plume's second centered moment, which is not necessarily a good measure of mixing. Some recent papers [7,8] highlight that one of the difficulties of extending these approaches to predicting mixing and mixing driven reactions lies in the ability to accurately capture mixing effects as quantified by the local mixing rate mentioned above [16,36,43], which are nonlinear in nature. Thus, the questions we pose to motivate this work is how much information, if any, about mixing one can actually attain solely from information on spreading?

Solute spreading and mixing are two different, but connected processes. Spreading quantifies the spatial extent of the solute, while mixing is a mechanical measure, which drives the dilution state and describes the degradation of gradients in concentration. While spreading characterizes the deformation and stretching of

* Corresponding author. Tel.: +1 574 631 0965.
E-mail address: bolster@nd.edu (D. Bolster).

a solute plume, increases in spreading can subsequently enhance mixing if a larger interfacial area develops between chemical species. In field studies, spreading is typically inferred through concentration breakthrough measurements, which are collected via tracer tests. This approach has been shown to be questionable when estimating mixing rates because concentration breakthrough curves are generally depth-averaged, implying that information on vertical concentration gradients vanishes [17,56,73,84]. Furthermore, a typical field site may have few measurement points (wells). Thus, even in the case where concentration is measured over a relatively small fluid volume, the spatial resolution of concentration data may allow one to approximate macrodispersion, but may be too low to evaluate mixing. Since spatial variations in concentrations and solute fluxes can be important controllers of reactive transport, one naturally wonders what physical mechanisms drive mixing and under which conditions breakthrough curves are valuable in the assessment of mixing.

Estimating transport parameters in heterogeneous velocity fields from calculated concentration breakthrough curves has been previously discussed [28,59,60,63] and found in several cases inaccurate in the determination of true mixing trends. Even for a relatively simple heterogeneity, this is evident: A recent numerical study by Luo and Cirpka [73] indicated that in an isotropic, homogeneous medium of high Peclet number with intermediate contrasts in permeability due to an elliptical inclusion, concentration breakthrough curves of reactive components can differ greatly from those of a calibrated numerical model.

Since variations in mixing are clearly related to complexities in porous media, previous work has been dedicated to understanding their fundamental relationship [17,24,35,39,70,71]. It has been shown that the even the simplest form of heterogeneity, such as discontinuities between segments of a porous medium, can lead to differences in mixing behavior: Sternberg [88] suggested that mixing is strongly driven by discontinuities in composite media between layered segments of glass beads in a one-dimensional column experiment, and recently Berkowitz et al. [13] concluded from lab experiments that even flow across a sharp interface between two differing media can dramatically affect solute transport depending on the direction of the flow. Cortis and Zoia [30] interpreted this phenomenon using a modified CTRW model. Appuhamillage et al. [3] numerically showed that for low Peclet number systems, asymmetries can exist in the flux-averaged breakthrough curves across a discontinuity, which Appuhamillage et al. [4] subsequently explained through the concept of an α -skew Brownian motion. Experiments by Castro-Alcala et al. [22] demonstrated clearly by use of image reflectometry that interfaces are regions of enhanced mixing as these interfaces can induce sharp gradients in solute concentration. Other interfaces, ubiquitous in hydrogeological contexts, such as saltwater intrusion systems [2,15,23,38,80,94] will also alter velocity fields and impact mixing. Also, interfaces with contrasts in permeability that are not directly perpendicular to flow direction are well known to cause refraction of streamlines [49].

Drawing inspiration from the simple setups of Berkowitz et al. [13] and Appuhamillage et al. [3,4], as well as the observations of Castro-Alcala et al. [22], we consider a very simple heterogeneity with the intent of studying possible links between spreading and mixing. It is a two-dimensional flow cell comprised of two homogeneous porous media of contrasting hydraulic properties separated by a sharp sloping interface. While this heterogeneity is incredibly simple, it allows us to probe several important features of flow with the goal of discerning their influence on mixing processes when considering a small, manageable number of dimensionless parameters. For example the presence of the sloping interface gives rise to features like flow focusing and defocusing, which have been shown to have a profound effect on mixing

[86,93]. Flow focusing regions correspond to regions of high velocity gradients; de Barros et al. [34] recently connected local mixing rates to the Okubo-Weiss parameter, a metric that quantifies local stretching and folding by velocity gradients. As noted our primary motivation for wanting to better understand mixing is that it is a primary driver of many chemical reactions (e.g. [7,8,10,16,36,37,73,92,19,42,25,26]). Without accurate and better understanding and descriptions of mixing, which can often be interpreted from conservative transport data, our capacity to understand and predict mixing driven reactions is limited.

The main interests of this work are to identify key drivers of mixing in addition to examining if breakthrough curves are useful in the assessment of mixing for the simple system presented when varying the characteristic Peclet number, flow direction, transverse dispersivity, and interface angle θ . In particular we probe for differences in mixing behavior when depth-averaged breakthrough curves are discernibly similar or situations where mixing is similar despite quite different spreading characteristics. This aims to give indications as to (i) instances in which concentration breakthrough curves reveal little information about true measures of mixing between the inlet and outlet of the flow cell, (ii) physical mechanisms that impact global and local mixing measures, and (iii) particular configurations where trends in mixing are not a function of the spreading. To study these important relations, we rely on numerical simulations of solute transport through the defined system.

2. System

The model considered in this work is schematically illustrated in Fig. 1: a two-dimensional domain of aspect ratio 10 comprised of two homogeneous porous media (e.g. made up of uniformly packed grains) separated by a sharp angled interface. Porosity is assumed constant throughout the whole domain.

We assume that hydraulic conductivity K_i and longitudinal dispersivity α_{Li} can be related through a characteristic grain diameter relationship, since hydraulic conductivity is often taken as proportional to grain diameter squared [54,55] and the longitudinal dispersivity for a uniform grain size can be assumed proportional to the characteristic grain diameter [20,21,44,81,96]. Therefore

$$K_i = Ad_i^2 \quad (1)$$

$$\alpha_{Li} = Bd_i \quad (2)$$

where A and B are constants; these relationships have been shown to be applicable to a uniformly packed homogeneous porous medium with a coefficient of uniformity equal to 1. With (1) and (2) contrasts between the flow and transport parameters of each medium are characterized entirely by contrasts in characteristic grain size.

2.1. Dimensionless parameters

The system presented can be described in terms of a finite number of dimensionless parameters. Three dimensionless parameters here largely control solute transport: θ , $\frac{d_1}{d_2}$ and $Pe_i = \frac{L_y}{\alpha_{Li}}$ where θ is the interface angle, d_i the characteristic grain size in domain i , Pe_i the Peclet number of domain i , where $i = 1$ and 2 , and L_y the width of the domain (Fig. 1). Subscripts 1 and 2 refer to the left and right porous medium, respectively. $\frac{d_1}{d_2}$ describes the grain size ratio, which reflects contrasts in hydraulic conductivity and dispersivity values. The Peclet number measures the ratio of advective to dispersive effects. In this study, media of high Peclet numbers are considered mainly to examine the role of the interface in affecting solute spreading and mixing as a function of θ . If the system were

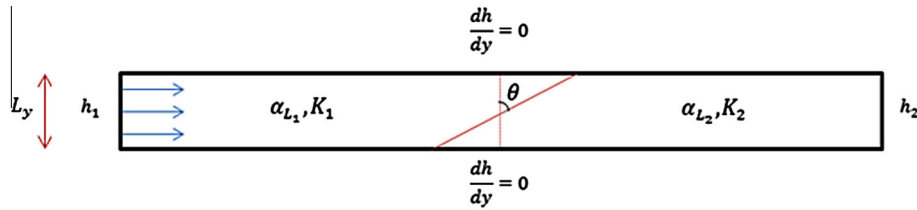


Fig. 1. Schematic of the numerical setup with boundary conditions and inherent properties. The longitudinal dispersivity, α_L , is the defined component here, while the transverse dispersivity, α_T , is specified as a certain percentage of α_L throughout the study.

dispersion dominated, the influence of the interface, which distorts the velocity field, is expected to be small.

2.2. Velocity field

The velocity field is solved using a cell-centered finite volume, two-point-flux-approximation, where the head h is obtained in two dimensions by combining Darcy’s Law and the continuity equation for steady state:

$$\nabla \cdot (K\nabla h) = 0. \tag{3}$$

The domain is discretized and fluxes are then calculated at the cell boundaries using cell-averaged values. Details of the numerical methods can be found in Aarnes et al. [1].

Figs. 2 and 3 show the magnitude of the computed pore water velocity fields for $\theta = 0, 30$, and 60 degrees for the coarse-to-fine and fine-to-coarse flow directions respectively. In all cases the outlet heads are set to zero and the inlet head is set to a constant such that the mean horizontal flow pore water velocity is equal to one. Note the velocity fields of the fine-to-coarse and coarse-to-fine flow directions are reflections of one another. This is because the direction of flow is simply reversed (Fig. 3).

3. Transport

The transport of a non-sorbing solute in a porous medium is modeled using the traditional advection–dispersion equation (ADE):

$$\frac{\partial c}{\partial t} + \nabla \cdot (\mathbf{u}c) = \nabla \cdot (\mathbf{D}\nabla c) \tag{4}$$

where \mathbf{u} is the seepage velocity and c the concentration of a conservative solute. In the coordinate system perpendicular to flow, the diagonal hydrodynamic dispersion tensor is assumed to be given by Bear [9]:

$$D_{ij} = \delta_{ij}\alpha_T|\mathbf{u}| + (\alpha_L - \alpha_T)u_i u_j / |\mathbf{u}| \tag{5}$$

where α_L and α_T are the longitudinal and transverse dispersivity, respectively. Molecular diffusion is neglected in this study because only advection-dominated systems are considered.

The random walk particle tracking method (RWPT) is used to numerically solve the ADE. RWPT offers a mass conservative, numerical-dispersion-free procedure in the simulation of solute transport. It is based on the analogy between the random walk Langevin equation and the Fokker-Plank equation for diffusion [58,62]. We consider the methodology presented by LaBolle et al. [65,66] to handle transport across discontinuous media. When dispersion is anisotropic, assuming porosity is constant within the flow cell, the discrete-time random walk is given by:

$$x_i(t - \Delta t) = x_i(t) + u_i(\mathbf{x}, t)\Delta t + \frac{1}{2} \sum_{j,k} B_{ijk}(\mathbf{x} + \Delta \hat{\mathbf{y}}, t)\Delta W_j + \frac{1}{2} \sum_{j,k,m,n} Z_{imn}(\mathbf{x}, t)B_{mjk}(\mathbf{x} + \Delta \mathbf{U}_n, t)\Delta W_j \tag{6}$$

where

$$\Delta \hat{\mathbf{y}}_l = \sum_{m,n} B_{lmn}(\mathbf{x}, t)\Delta W_m$$

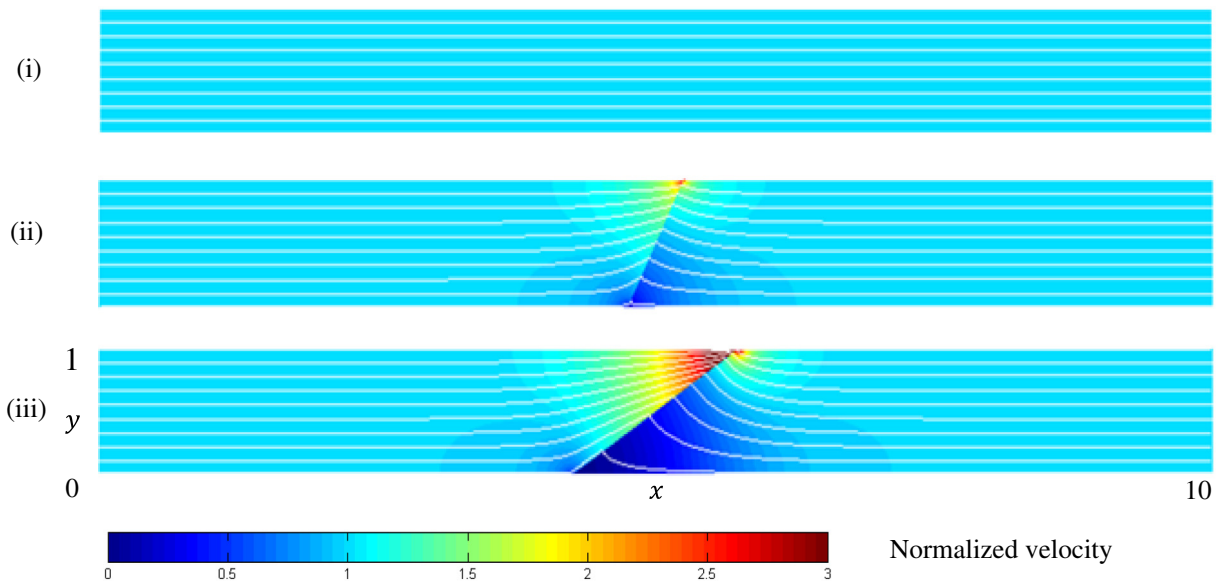


Fig. 2. The magnitude of the velocity field for $Pe 10^2-10^3$ (coarse-to-fine media) where: (i) $\theta = 0$ degrees, (ii) $\theta = 30$ degrees, and (iii) $\theta = 60$ degrees. Both components of the velocity field are normalized by \bar{u}_x and streamlines are shown in white. Note that the velocity field colorbar is truncated at a maximum velocity of 3 to better visualize velocity contrasts.

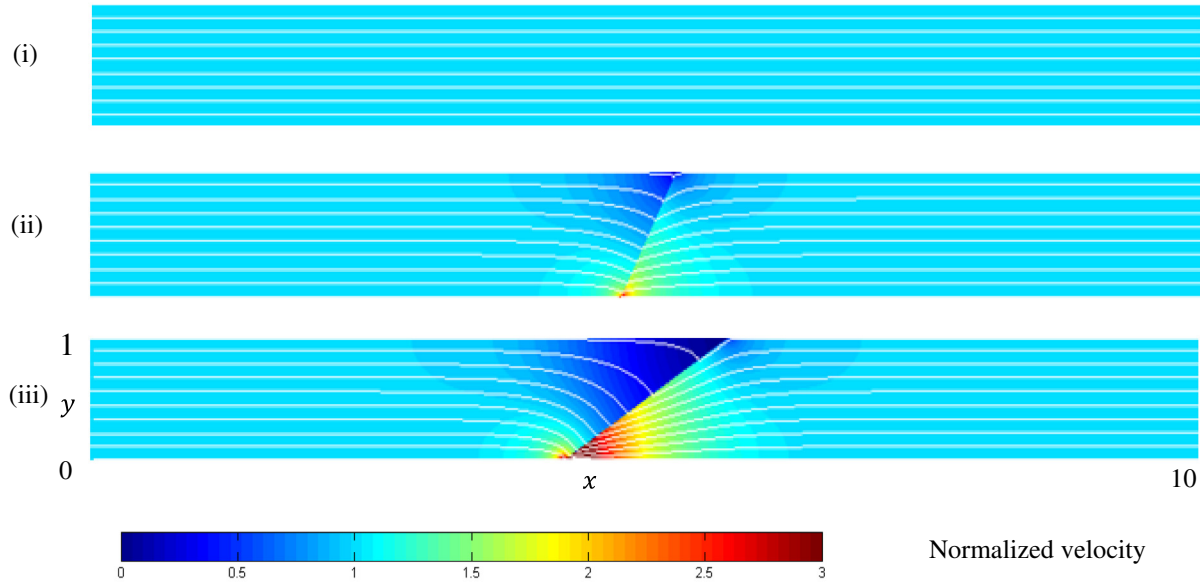


Fig. 3. The magnitude of the velocity field for $Pe\ 10^3\text{--}10^2$ (fine-to-coarse media) where: (i) $\theta = 0$ degrees, (ii) $\theta = 30$ degrees, and (iii) $\theta = 60$ degrees. Note that the velocity field colorbar is truncated at a maximum velocity of 3 to better visualize velocity contrasts.

$$B_{ijk}(\mathbf{x}, t) = \lambda_k^{\frac{1}{2}}(\mathbf{x}, t) Z_{ijk}(\mathbf{x}, t)$$

$$Z_{imn}(\mathbf{x}, t) = [e_n(\mathbf{x}, t)]_i [e_n(\mathbf{x}, t)]_m$$

$$\Delta U_{nl} = \lambda_n^{\frac{1}{2}}(\mathbf{x}, t) \Delta W_l$$

$$\Delta W_j = \xi_j \sqrt{\Delta t}$$

and $i, j, k, l, m, n = 1, 2$ for a two dimensional system. ξ_j is a standard normal random variable of zero mean, unit variance and $e_n(\mathbf{x}, t)$ is the eigenvector corresponding to λ_n , the n th eigenvalue of the dispersion tensor $\lambda_1(\mathbf{x}, t) = 2D_L$, $\lambda_2(\mathbf{x}, t) = 2D_T$. This method is based on evaluating the advective displacement at the current particle position with the dispersive displacement recalculated at an intermediate step, representing the current position summed with the initial dispersive displacements; this circumvents the calculation of gradients in dispersion to maintain similarity between the Fokker-Plank and advection dispersion equations. Further details can be found in LaBolle et al. [66], Lim [72], and LaBolle and Zhang [67]. To filter noise, all concentration and concentration gradient fields are calculated using a kernel regression method (Takeda et al. [90], Fernández-García and Sanchez-Vila [47]).

3.1. Measures of mixing

To study mixing at the local scale, we consider the mixing factor, presented by Pope [82] and that arises naturally in the context of mixing driven reactions (De Simoni et al. [36]):

$$f_{mix} = \nabla^T c(\mathbf{x}, t) \mathbf{D} \nabla c(\mathbf{x}, t) \quad (7)$$

where f_{mix} can be thought of as a measure of dispersive flux. Eq. (7) is clearly related to the concentration variability within a solute plume, which can be pronounced in heterogeneous porous media with complex flow fields [17,18,22,35,70]. Increases in spreading can often lead to more dispersive mass transfer, and thus enhanced mixing [41,70].

In addition, we consider the dilution index [63] as a global measure of mixing. The dilution index characterizes the overall mixing

state and measures the apparent volume occupied by a solute; it is given by

$$E(t) = e^{-\int_V p \ln(p) dV} \quad (8)$$

where

$$p(\mathbf{x}, t) = \frac{c(\mathbf{x}, t)}{\int_V c(\mathbf{x}, t) dV}$$

is the normalized concentration. V is the volume of the domain. Large values of $E(t)$ represent well-mixed systems where the solute is more uniformly dispersed and the maximum concentration is reduced. The dilution index helps one distinguish between dilution and macrodispersive spreading, which for many systems are not identical [60,63]. The concept has recently been extended to reactive systems [25]. Note that the mixing factor derived by De Simoni et al. [36] is consistent with the dilution index proposed by Kitaniadis [63], as an increase in the system entropy, driven by an increase in the volume occupied by the solute, implies that concentration gradients are smoothed and the system is more well-mixed [41].

We also studied the scalar dissipation rate [70], a spatially integrated measure of the local mixing factor (10). These results are not presented here, as the behaviors of the dilution index and scalar dissipation rate are analogous, providing little additional insight. This is unsurprising as the two metrics are closely related [36,37] and evolve in very similar manners (e.g. [18]).

For all simulations numerical grids were refined while time steps were reduced and particle numbers increased until further refinement altered measured values of the dilution index by less than 0.1% based on an L2 norm relative error [83]. Acceptable convergence typically occurred with a spatial grid resolution of $dx = 0.01$ and half a million random walk particles, although for convergence testing we also ran simulations with $dx = 0.001$ and as many as 40 million particles.

4. Results and discussion

In all simulations conservative particles are tracked through time and space by relations (6). Initially at $t = 0$, the particles are uniformly distributed across the y -dimension at the inlet ($x = 0$)

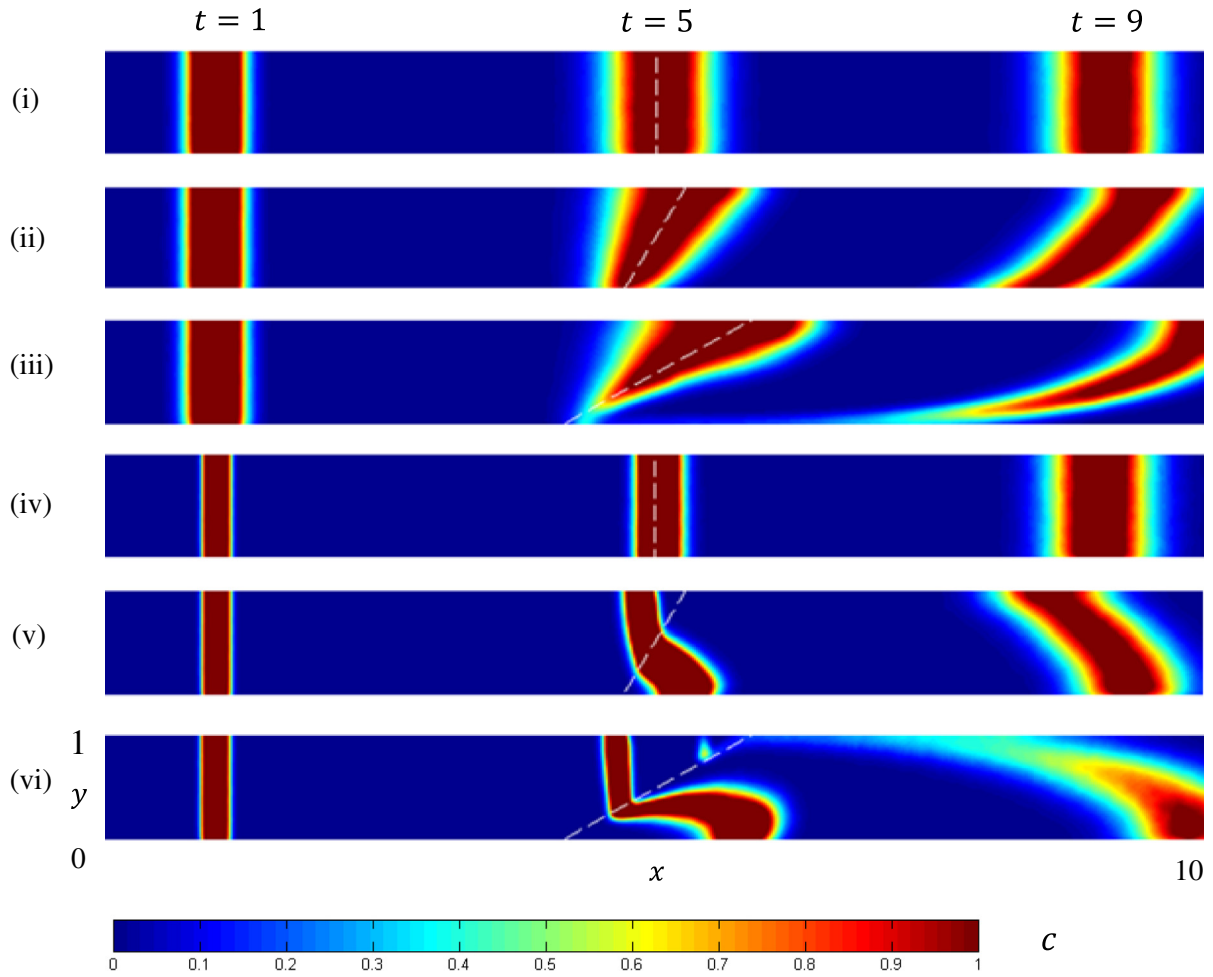


Fig. 4. Snapshots of concentration fields for $\alpha_T = 0.2\alpha_L$ at $t = 1, 5$, and 9 , where: (i) $\theta = 0^\circ$, (ii) $\theta = 30^\circ$, (iii) $\theta = 60^\circ$, coarse-to-fine media; and (iv) $\theta = 0^\circ$, (v) $\theta = 30^\circ$, (vi) $\theta = 60^\circ$, fine-to-coarse media. The Peclet number is $Pe = 10^2$ (coarse) and 10^3 (fine). Distortion of the plume and enhanced spreading by the angled interface is clearly evident.

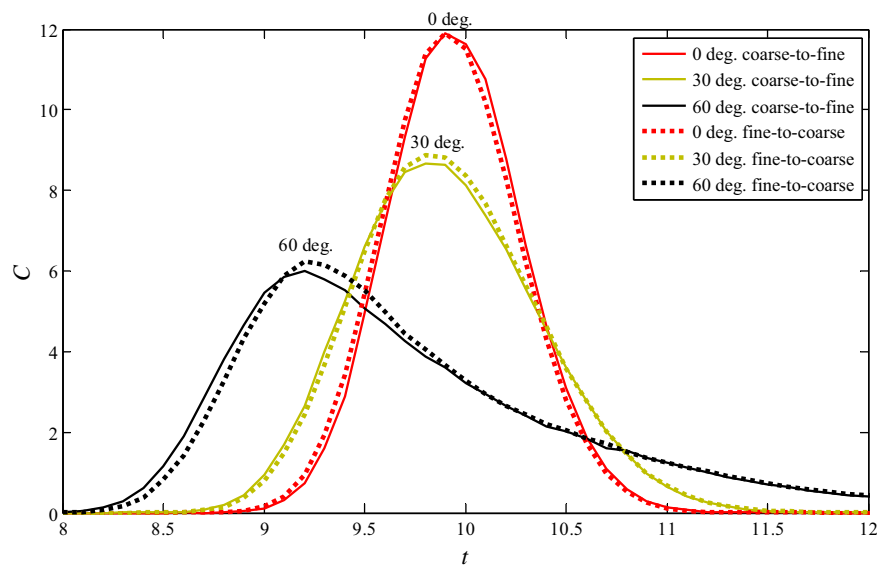


Fig. 5. Vertically-averaged concentration breakthrough curves calculated at the outlet for flow from Peclet number 10^2 – 10^3 (coarse-to-fine media) and 10^3 – 10^2 (fine-to-coarse media), where $\alpha_T = 0.2\alpha_L$. Differences in the concentration breakthrough curves are predominantly driven by differences in the interface angle, θ .

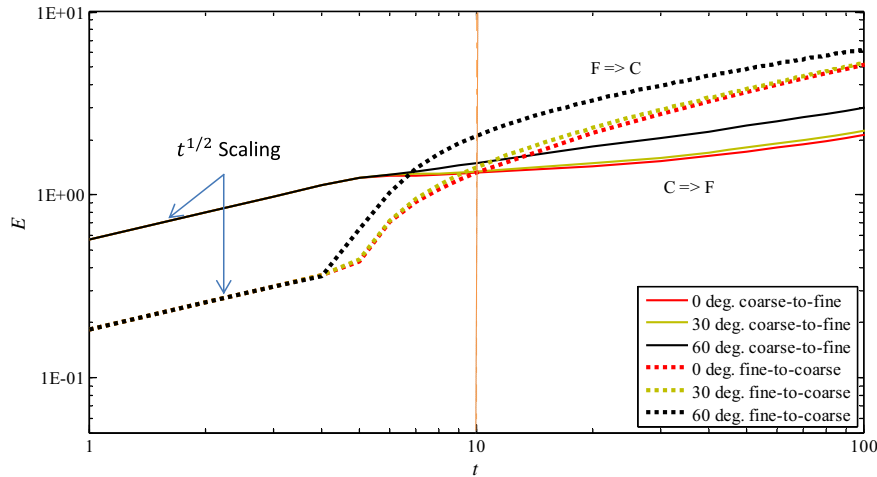


Fig. 6. Dilution indices for flow from $Pe\ 10^2\text{--}10^3$ (coarse-to-fine media; $C \Rightarrow F$) and $10^3\text{--}10^2$ (fine-to-coarse media; $F \Rightarrow C$), where $\alpha_T = 0.2\alpha_L$.

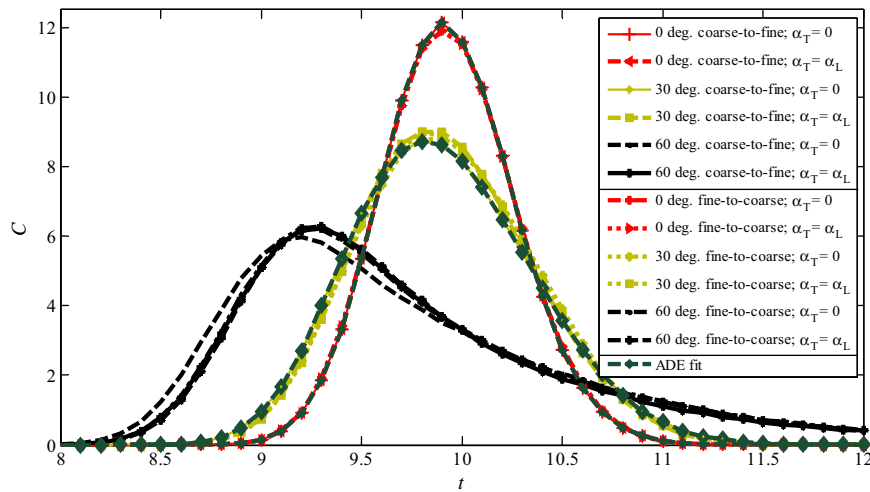


Fig. 7. Vertically averaged breakthrough curves for flow from $Pe\ 10^2\text{--}10^3$ (coarse-to-fine media) and $10^3\text{--}10^2$ (fine-to-coarse media), where $\alpha_T = 0$ and $\alpha_T = \alpha_L$. Fitted solutions to the one-dimensional ADE are given in green for the 0 and 30 degree case. (For interpretation of the references to color in this figure legend, the reader is referred to the web version of this article.)

to represent a line source initial condition. In this discussion, results corresponding to media with grain size ratios of $d_1/d_2 = 0.1$ (“fine to coarse”) or 10 (“coarse to fine”) are considered. The media for these cases have Pe numbers of 10^2 (coarse medium) and 10^3 (fine medium). These are chosen to highlight central observations; we conducted a comprehensive study that spanned values across the spectrum of $10 < Pe < 10^4$ with grain diameter contrasts d_1/d_2 up to 1000. We found all cases to behave in a comparable manner with similar observations to those we highlight here. As noted we focus exclusively on advection-dominated systems and thus smaller Pe values are not included.

In Section 4.1, we consider the case $\alpha_T/\alpha_L = 0.2$, which is a commonly assumed value [52,11,87]; for the chosen Peclet numbers this should be reasonable, but it is important to note that this ratio can depend on Peclet number. In Sections 4.2 and 4.3, cases where $\alpha_T = 0$ as well as $\alpha_T = \alpha_L$ are also considered. These two values are chosen, because $\alpha_T = 0$ is a value often taken in analytical solutions (e.g. Fernandez-Garcia et al. [48], who studied mixing driven reactions in a stratified aquifer) and likewise many previous studies have considered the case of $\alpha_T = \alpha_L$ or indeed constant dispersion coefficient (e.g., [70]). We also choose these extreme values in order to gain a broader understanding of the impact of transverse dispersion on mixing.

4.1. Similarities in spreading: the importance of flow direction

Displayed in Fig. 4 are concentration fields for three considered values of θ at three distinct times for the coarse-to-fine and fine-to-coarse flow directions respectively. Fig. 5 shows depth-averaged concentration breakthrough curves measured at the outlet of the flow cell with both flow directions considered and θ equal to 0, 30, and 60 degrees. From Figs. 4 and 5, it is clear that increasing θ results in progressively enhanced spreading, characterized by earlier arrivals, broader distributions of arrival times and lower concentration peaks. When examining the spatial distribution of concentration and concentration breakthrough curves of $\theta = 30$ and $\theta = 60$ degrees, it is clear that broader arrival time distributions arise as θ progressively increases because velocity components can vary considerably near the interface (see Figs. 2 and 3). Note that reversing the direction of flow does not appear to significantly impact the breakthrough curves. Only minute differences exist in the curves presented in Fig. 5 between alternate flow directions with identical interface angles. This is presumably a reflection of the fact that particles statistically sample the almost same velocity fields independent of direction (see Figs. 2 and 3). The main interest here is to highlight the discernible differences in spreading, which are demonstrated by lower concentration peaks and broader arrival

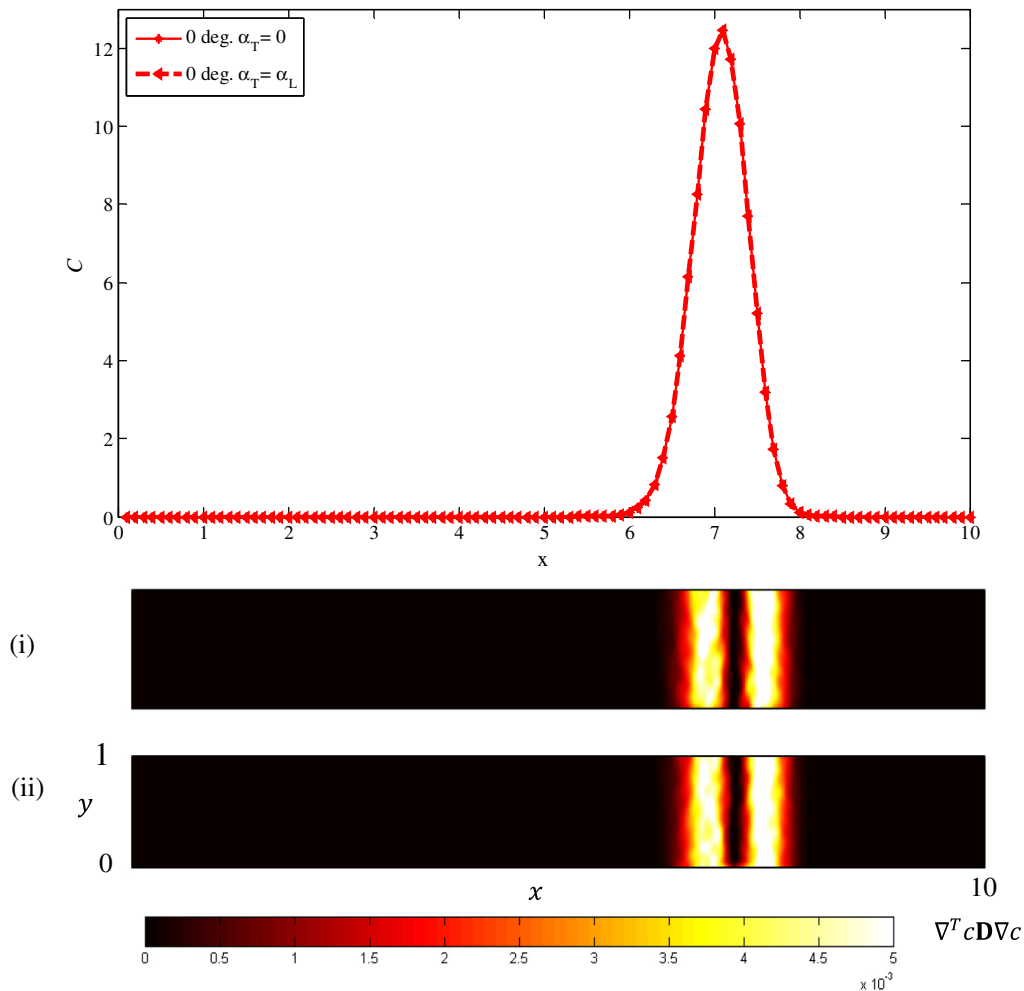


Fig. 8. Horizontal concentration profile (top), and mixing rate, f_{mix} (bottom, i–ii), for $\theta = 0$ degrees, $t = 7$, and the following transverse dispersivities: (i) $\alpha_T = 0$; (ii) $\alpha_T = \alpha_L$. The concentrations are clearly independent of α_T .

time distributions, as exhibited clearly in Fig. 5 when varying θ . Noting that concentration breakthrough curves are nearly identical between reversed flow directions for a given θ is important because effective transport parameters calibrated solely on concentration breakthrough data would be similar [28].

Global mixing trends, as quantified by the dilution index (11), $E(t)$, are shown in Fig. 6. As expected the dilution index grows with time, indicative of the monotonic increase in the volume occupied by the solute with time, due to dispersion. Notice the growth rate of $E(t)$ before $t = 4$ scales like $t^{\frac{1}{2}}$ and reflects a constant spreading of the tracer. Disruptions in the dilution indices thereafter correspond to the time when the flow focusing caused by the interface is felt by the plume. For all calculations of the dilution index presented, particles that leave the domain through the right boundary continue to be tracked by assuming that they continue to move in a uniform horizontal velocity field. This is done to see how the dilution index would continue to evolve, but the primary focus in this work will be on the evolution before particles reach the right boundary.

Distinct global mixing trends exist when considering a reversal of the flow direction; after $t = 4$, dilution indices follow a trend dependent upon θ , where larger values of θ enhance dilution due to the solute occupying a larger area. A drop in the slope of $E(t)$ after $t = 4$, for all values of θ of the coarse-to-fine flow direction, is driven by the already disperse distribution reaching the fine medium, where the rate of change of the area occupied by the

solute is subsequently lowered. Alternatively, an increase in the dilution indices rate of growth occurs in the fine-to-coarse flow direction once the tracer begins entering the flow-focusing zone. The difference in time of the initial jumps can be attributed to the angle of the interface, where for $\theta = 60$ degrees especially, the high velocity zone distorts the solute plume at a slightly earlier time. Disruptions in the dilution indices due to the interface, for all values of θ , subsequently diminish and dilution rates return to a constant slope, scaling like $t^{\frac{1}{2}}$, at some given time. This reflects the fact that when the plume is completely within a homogeneous medium, transport returns to be one-dimensional and Fickian. Note $t = 10$, the mean arrival time based on average flow speed, in Fig. 6. Based on identical breakthrough curves, independent of the flow directions, one might expect the degree of mixing to be independent of flow direction as well. While it is clear that for the $\theta = 0^\circ, 30^\circ$ case this is approximately true there are notable differences for the $\theta = 60^\circ$ case, despite the fact that the breakthrough curves do not vary significantly with flow direction (Fig. 5).

4.2. Role of transverse dispersion on mixing when $0 \leq \alpha_T \leq \alpha_L$

In this section and the following we explore the role of transverse dispersivity, a quantity that can be highly uncertain in practice (e.g. see the discussion in [14]), but well known to impact mixing in a dominant and important manner [24]. Consider Fig. 7, where vertically-averaged concentration breakthrough curves

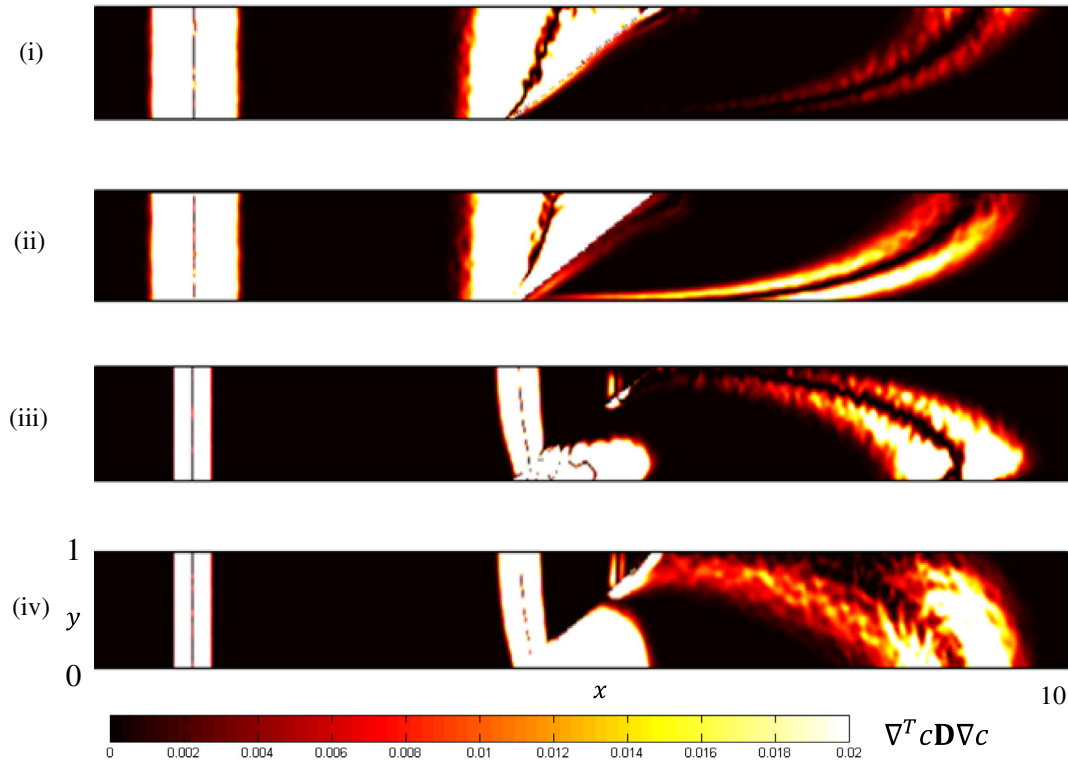


Fig. 9. Temporal evolution of the mixing rate, f_{mix} , for $\theta = 60$ degrees at $t = 1, 4.5, 8$. (top) Coarse-to-fine media, ($Pe 10^2-10^3$), where (i) $\alpha_T = 0$; (ii) $\alpha_T = \alpha_L$; (bottom) fine-to-coarse media ($Pe 10^3-10^2$), where (iii) $\alpha_T = 0$; (iv) $\alpha_T = \alpha_L$.

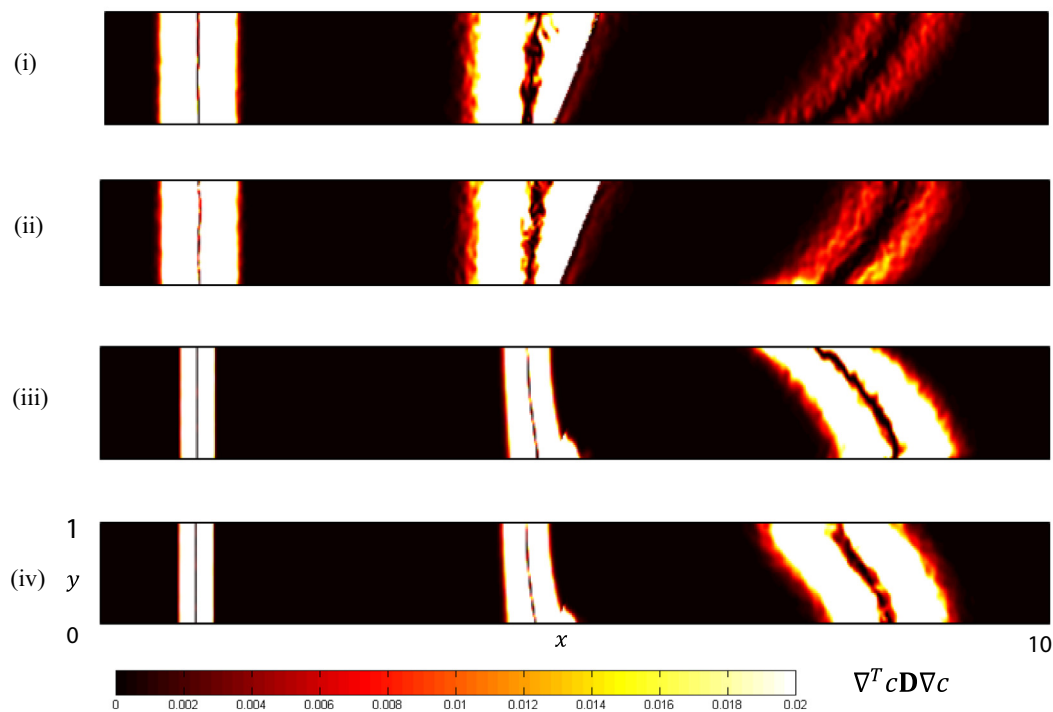


Fig. 10. Temporal evolution of the mixing rate, f_{mix} , for $\theta = 30$ degrees at $t = 1, 4.5, 8$. (top) Coarse-to-fine media, ($Pe 10^2-10^3$), where (i) $\alpha_T = 0$; (ii) $\alpha_T = \alpha_L$; (bottom) fine-to-coarse media ($Pe 10^3-10^2$), where (iii) $\alpha_T = 0$; (iv) $\alpha_T = \alpha_L$.

measured at the outlet are displayed for all angles and both flow directions, with $\alpha_T = 0$ and $\alpha_T = \alpha_L$. It is evident that small differences can occur when $\alpha_T = \alpha_L$ as θ becomes progressively

larger. However these changes are very small and the breakthrough curves are nearly identical to those presented in Fig. 5, implying that the specific value of α_T does not significantly impact

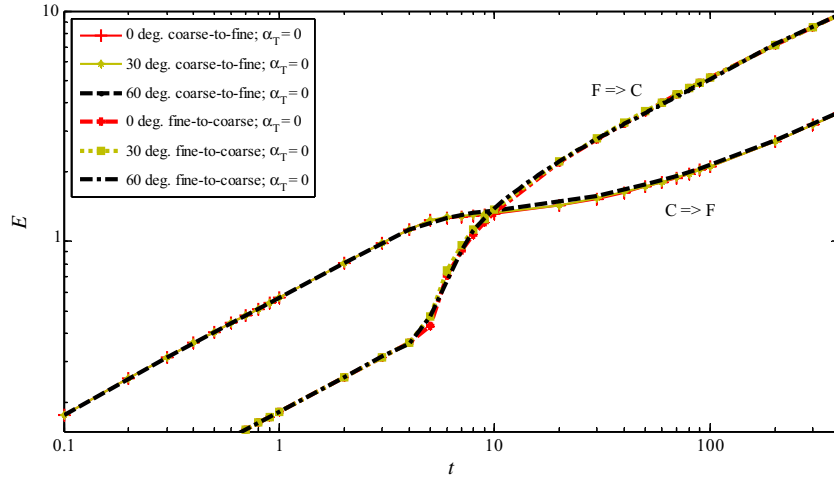


Fig. 11. Dilution indices for $\theta = 0, 30,$ and 60 degrees for the fine-to-coarse ($F \Rightarrow C$) and coarse-to-fine ($C \Rightarrow F$) flow directions where $\alpha_T = 0$.

Table 1

Qualitative summary of the dependencies in the system. For example, the dependence of the BTC on θ is strong, regardless of α_T .

Dependence of/on	System parameters	
	Interface slope, θ	Flow direction
Breakthrough curves (BTC)	Strong dependence	Very weak (for $\alpha_T = 0$)/weak (for $\alpha_T = \alpha_L$)
Dilution Index	Weak (for $\alpha_T = 0$)/significant (for $\alpha_T = \alpha_L$)	Strong dependence

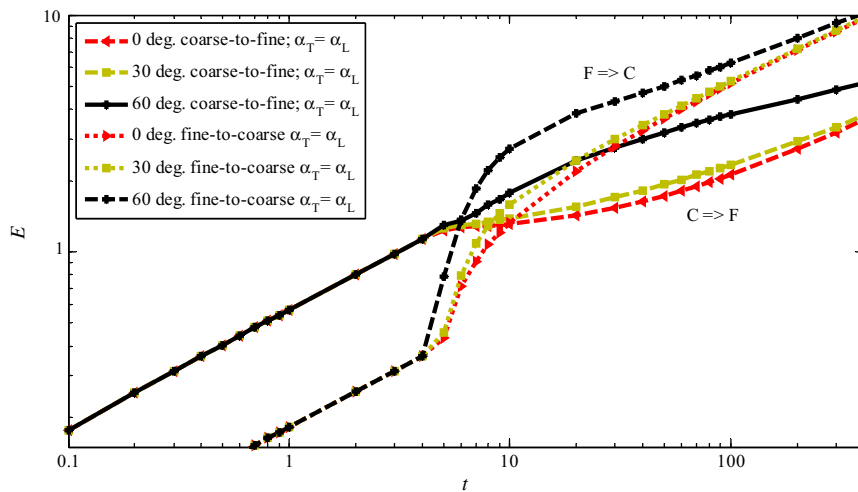


Fig. 12. Dilution indices for $\theta = 0, 30,$ and 60 degrees for the fine-to-coarse ($F \Rightarrow C$) and coarse-to-fine ($C \Rightarrow F$) flow directions where $\alpha_T = \alpha_L$.

concentration breakthrough measurements. Fitted solutions of the one-dimensional advection dispersion equation (ADE) are also shown for the 0 and 30 degree case, where the effective dispersion coefficient for the 30 degree case is approximately double the 0 degree case. This result will be discussed in greater detail in Section 4.3. A fit of the ADE to the 60 degree case is not presented, because while performed it is not a particularly good one.

Fig. 8 shows the depth-averaged concentration profile at $t = 7$ and local mixing calculations (f_{mix}) for the coarse-to-fine flow direction where $\theta = 0$ degrees. It is clear that when examining the overlying horizontal concentration profile the local mixing factor is zero at the plume center because no gradients in concentration exist in the horizontal and transverse direction [36]. Notice that the local mixing rates for $\theta = 0$ degrees are independent of the

value of α_T as one would expect because no transverse gradients in concentration should exist.

Consider now the comparison of the local mixing factor f_{mix} from Eq. (10) between coarse-to-fine and fine-to-coarse flow directions of $\theta = 60$ degrees at three distinct times in Fig. 9. Examining images (i) and (ii) in Fig. 9, it is evident that differences in the mixing rate exist, due to differences in transverse dispersivity, most notably near and past the interface. Mixing is additionally enhanced in images (iii) and (iv) due to the specified flow direction; higher concentration gradients inherent in the fine media, leading up to the interface, allow for transverse dispersion to more greatly impact mixing slightly after the interface where streamlines diverge. Differences between images (i) and (ii), in addition to (iii) and (iv) are distinct after the interface where amplified transverse

mixing is present. An enhanced area of mixing just above the interface in the fine-to-coarse direction for image (iv) and less so for image (iii), at $t = 8$, is not seen in the reversed flow direction (images (i) and (ii)). Notice also that around the center of the concentration distribution, localized zones of non-mixing persist throughout time even when the interface distorts and stretches the solute plume. Similar results have been identified for a variety of other Peclet number ratios. In regions near the interface, where flow focusing occurs, heightened transverse dispersivity acts to enhance mixing in image (ii) where the distance between streamlines is diminished, complimenting results discussed in previous works [86,93]. Note however the role of transverse dispersion in the flow defocusing zone in image (iv), especially just after the interface, where high mixing rates are observed in comparison to image (iii). Also observe that at late times, the stretched plume allows for transverse dispersion to enhance mixing rates at the plume edges.

4.3. Similarities in mixing

Fig. 10 is similar to Fig. 9, but for $\theta = 30$ degrees. Unlike the $\theta = 60$ case, there is a much weaker dependence of local mixing rate on α_T . The reason for this seems to lie in the fact that the interface causes the plume to only rotate slightly meaning that vertical concentration gradients are relatively small. Corresponding dilution indices are shown in Fig. 11 ($\alpha_T = 0$) and 12 ($\alpha_T = \alpha_L$). For the case with no transverse dispersion, global mixing trends, as quantified by the dilution index, are virtually identical for all interface angles as clearly shown in Fig. 11. This result is quite remarkable given the strong and discernible differences in spreading as observed in the breakthrough curves in Fig. 5. These results have strong implications for quantifying mixing in situations where transverse dispersion is much smaller than longitudinal dispersion and truly highlights the critical role that transverse dispersion plays in mixing as suggested by previous authors (e.g. [93]). The results are summarized briefly in Table 1.

In Figs. 6 and 12, where transverse dispersion is present, clear and different global mixing trends emerge for different interface angles. The differences between the 0 and 30 degree cases, while discernible are not that large and not as large as one might expect from the differences in spreading as shown in the breakthrough curves of Fig. 5. This is likely because the 30 degree case, while distorting the uniform velocity field, does not appear to distort it rotationally all that significantly; rotation, or better said velocity gradients and vorticity is critical to the enhancement of mixing rates as shown by de Barros et al. [34].

5. Conclusions

In this work we numerically probe for specific drivers of mixing and question the relationship between spreading and mixing. We consider solute transport through a very simple heterogeneous porous medium in an advection-dominated context: a flow cell comprised of two homogeneous media separated by a sharp, angled interface. From this study we draw several broad conclusions, which may have practical implications for more complex heterogeneous systems:

- Vertically averaged breakthrough curves provide relatively little valuable information about mixing:
 - Flow direction matters for mixing. For this configuration nearly identical breakthrough curves can be obtained for fine to coarse or coarse to fine flow directions, which in terms of an effective model would provide virtually identical fitting parameters, while mixing patterns and rates can be quite

different. This may have important implications for remediation efforts, where enhanced mixing may be desirable; e.g. imagine a remediation process that requires injection and mixing of a treatment solution between two wells (i.e. the boundaries of our numerical domain). In this system it could be preferable to inject this solution in one specific well and extract from the other instead of the other way around, even though this would not be discernible from breakthrough curve results alone.

- Spreading, as inferred by fitting the depth averaged breakthrough curves to the ADE, can suggest greater degrees of mixing than actually observed. Thus one must be cautious inferring mixing rates from effective parameters obtained from depth averaged breakthrough curves.

These conclusions are consistent with the observations of Luo and Cirpka [73], who studied predictability of mixing driven reactions from calibration of model parameters to vertically averaged breakthrough curves.

- Accurate knowledge of transverse dispersivity is critical to predicting mixing accurately.
 - Breakthrough curves for the systems studied here are relatively insensitive to transverse dispersion. Only small differences in breakthrough curves are observed as transverse dispersivity is changed all the way from 0 to a maximum value equal to longitudinal dispersivity. Any small changes that are observed only occur for the most heterogeneous case considered, i.e. the 60 degree interface angle. This suggests that, even with detailed knowledge of the heterogeneity, vertically averaged breakthrough curves do not provide valuable information that could be used to accurately quantify transverse dispersivity.
 - By contrast mixing rates, as quantified by the dilution index, are extremely sensitive to transverse dispersivity. When we set transverse dispersivity to zero the temporal evolution of the dilution index was very similar and independent of interface angle. This is despite the fact that increased interface angles lead to significantly different spreading, which one might expect to suggest greater mixing. As the transverse dispersivity is increased from zero discernible differences in dilution index emerge.

This is consistent with the idealized predictions of Bolster et al. [18] and more general theory of de Barros et al. [34], whose local analytical expressions for the evolution of the dilution index clearly demonstrate the dependence on transverse dispersion for enhanced mixing. It further demonstrates the critical need to better evaluate transverse dispersivity values, which are known to be quite uncertain [14]. It is also well known that flow focusing, or convergence of streamlines, can significantly enhance mixing [93]. The mechanism for this is that as streamlines get closer, both the concentration gradients and velocity increase, and transverse dispersion is enhanced. In other words, as streamlines get closer, it is easier for solute particles to traverse them. This enhanced mixing mechanism is clearly driven by transverse dispersion and our results highlight and reinforce this critical point.

Our work demonstrates that while there may be links between spreading (as inferred from a depth averaged breakthrough curve) and mixing of solutes (as quantified by the dilution index), which has received much previous attention, the connection between the two is not an obvious one and highly sensitive to transverse dispersivity, which it is practically impossible to infer from a depth averaged breakthrough curve. In particular we demonstrate using a very simple form of heterogeneity that systems with identical

spreading can have quite different mixing and systems with very different spreading can have very similar mixing.

It is important to note that the results obtained here assume that the conditions imposed for flow and transport across the interface are the correct ones, i.e. that the method of LaBolle et al. [66] and Eq. (9) reflect the physics of transport across the interface correctly. This is a currently conventional and accepted model for such transport. However, there is experimental evidence that for smaller Peclet number systems these may not be correct [13] and that other conditions may be appropriate [30]. However for the large Peclet numbers considered here the evidence from these studies suggest any problem associated with this condition should be small. This is an issue we are currently further exploring experimentally in our research group. Likewise the initial and boundary conditions, corresponding to a linear flood condition, which was motivated by the observations of [13] and [4], obviously play an important role in our observations and so caution must be taken in extrapolating any conclusions.

Acknowledgements

BS would like to thank Ricky Villarreal for helpful discussions and assistance throughout the course of this work. We also would like to thank Dr. Tim Ginn and two anonymous reviewers for helpful review comments. This work was supported via NSF grant EAR-1113704.

References

- [1] Aarnes JE, Gimse T, Lie KA. An introduction to the numerics of flow in porous media using Matlab. In: Hasle G, Lie K-A, Quak E, editors. Geometric modelling, numerical simulation, and optimization: applied mathematics at SINTEF. Berlin/Heidelberg: Springer; 2007. p. 261–302.
- [2] Abarca E, Carrera J, Sánchez-Vila X, Dentz M. Anisotropic dispersive Henry problem. *Adv Water Res* 2007;30(4):913–26.
- [3] Appuhamillage TA, Bokil VA, Thomann E, Waymire E, Wood BD. Solute transport across an interface: a Fickian theory for skewness in breakthrough curves. *Water Resour Res* 2010;46(W07511):13.
- [4] Appuhamillage TA, Bokil VA, Thomann E, Waymire E, Wood BD. Occupation and local times for skew Brownian motion with applications to dispersion across an interface. *Ann Appl Probab* 2011;21(1):183–214.
- [5] Ayora C, Taberner C, Saaltink MW, Carrera J. The genesis of dedolomites: a discussion based on reactive transport modeling. *J Hydrol* 1998;209(1/4):346–65.
- [6] Auriault J, Adler P. Taylor dispersion in porous media: analysis by multiple scale expansions. *Adv Water Resour* 1995;18:217–26.
- [7] Battiato I, Tartakovsky DM, Tartakovsky AM, Scheibe TD. On breakdown of macroscopic models of mixing-controlled heterogeneous reactions in porous media. *Adv Water Resour* 2009;54(2):243–55.
- [8] Battiato I, Tartakovsky DM. Applicability regimes for macroscopic models of reactive transport in porous media. *J Contam Hydrol* 2011;120:18–26.
- [9] Bear J. Dynamics of fluids in porous media. N.Y.: Elsevier; 1972.
- [10] Benson DA, Meerschaert MM. Simulation of chemical reaction via particle tracking: diffusion-limited versus thermodynamic rate-limited regimes. *Water Resour Res* 2008;44(12).
- [11] Bergeron MP, Freeman EJ. Estimating groundwater concentrations from mass releases to the aquifer at the integrated disposal facility and tank farms in the Hanford Central Plateau. PNNL-14891, Pacific Northwest National Laboratory, Richland, Washington, 2005.
- [12] Berkowitz B, Cortis A, Dentz M, Scher H. Modeling non-Fickian transport in geological formations as a continuous time random walk. *Rev Geophys* 2006;44(2).
- [13] Berkowitz B, Cortis A, Dror I, Scher H. Laboratory experiments on dispersive transport across interfaces: the role of flow direction. *Water Resour Res* 2009;45.
- [14] Bijeljic B, Blunt MJ. Pore-scale modeling of transverse dispersion in porous media. *Water Resour Res* 2007;43(W12S11):48–96. <http://dx.doi.org/10.1029/2006WR005700>.
- [15] Bolster Diogo T, Tartakovsky Daniel M, Dentz Marco. Analytical models of contaminant transport in coastal aquifers. *Adv Water Resour* 2007;30(9):1962–72.
- [16] Bolster D, Benson DA, Le Borgne T, Dentz M. Anomalous mixing and reaction induced by superdiffusive nonlocal transport. *Phys Rev E* 2010;82(2):021119.
- [17] Bolster D, Valdés-Parada FJ, Le Borgne T, Dentz M, Carrera J. Mixing in confined stratified aquifers. *J Contam Hydrol* 2011;120–121:198–212.
- [18] Bolster D, Dentz M, Le Borgne T. Hypermixing in linear shear flow. *Water Resour Res* 2011;47:W09602.
- [19] Bolster D, de Anna P, Benson DA, Tartakovsky AM. Incomplete mixing and reactions with fractional dispersion. *Adv Water Resour* 2012;37:86–93.
- [20] Bromly M, Hinz CL, Aylmore AG. Relation of dispersivity to properties of homogeneous saturated repacked oil columns. *Eur J Soil Sci* 2007;58(1):293–301.
- [21] Carberry JJ, Bretton RH. Axial dispersion of mass in flow through fixed beds. *AIChE J* 1958;4(3):367–75.
- [22] Castro-Alcala E, Fernandez-Garcia D, Carrera J, Bolster D. Visualization of mixing processes in a heterogeneous sand box aquifer. *Environ Sci Technol* 2012;46:3228–35.
- [23] Chang SW, Clement TP. Laboratory and numerical investigation of transport processes occurring above and within a saltwater wedge. *J Contam Hydrol* 2013;147:14–24.
- [24] Chiogna G, Cirpka OA, Grathwohl P, Rolle M. Transverse mixing of conservative and reactive tracers in porous media: quantification through the concepts of flux-related and critical dilution indices. *Water Resour Res* 2011;47:W02505.
- [25] Chiogna G, Hochstetler DL, Bellin A, Kitanidis PK, Rolle M. Mixing, entropy and reactive solute transport. *Geophys Res Lett* 2012;39:L20405.
- [26] Chiogna G, Bellin A. Analytical solution for reactive solute transport considering incomplete mixing within a reference elementary volume. *Water Resour Res* 2013;49:2589–600.
- [27] Chrysikopoulos CV, Roberts PV, Kitanidis PK. One-dimensional solute transport in porous media with partial well-to-well recirculation: application to field experiments. *Water Resour Res* 1990;26(6):1189–95.
- [28] Cirpka OA, Kitanidis PK. Characterization of mixing and dilution in heterogeneous aquifers by means of local temporal moments. *Water Resour Res* 2000;36(5):1209–20.
- [29] Cirpka OA, Valocchi AJ. Two-dimensional concentration distribution for mixing-controlled bioreactive transport in steady state. *Adv Water Resour Res* 2007;30(6–7):1668–79.
- [30] Cortis A, Zoia A. Model of dispersive transport across sharp interfaces between porous materials. *Phys Rev E* 2009;80:011122.
- [31] Dagan G. Solute transport in heterogeneous porous formations. *J Fluid Mech* 1984;145:151–77.
- [32] Dagan G. Time-dependent macrodispersion for solute transport in anisotropic heterogeneous aquifers. *Water Resour Res* 1988;24(9):1491–500.
- [33] Dagan G. Flow and transport in porous formations. Springer Verlag; 1989.
- [34] de Barros FJP, Dentz M, Koch J, Nowak W. Flow topology and scalar mixing in spatially heterogeneous flow fields. *Geophys Res Lett* 2012;39:L08404. <http://dx.doi.org/10.1029/2012GL051302>.
- [35] De Dreuzy J-R, Carrera J, Dentz M, Le Borgne T. Time evolution of mixing in heterogeneous porous media. *Water Resour Res* 2012;48:W06511.
- [36] De Simoni M, Carrera J, Sánchez-Vila X, Guadagnini A. A procedure for the solution of multicomponent reactive transport problems. *Water Resour Res* 2005;41:W11410.
- [37] De Simoni M, Sanchez-Vila X, Carrera J, Saaltink MW. A mixing ratios-based formulation for multicomponent reactive transport. *Water Resour Res* 2007;43:W07419.
- [38] Dentz M, Tartakovsky DM, Abarca E, Guadagnini A, Sanchez-Vila X, Carrera J. Variable-density flow in porous media. *J Fluid Mech* 2006;561(1):209–35.
- [39] Dentz M, Carrera J. Mixing and spreading in stratified flow. *Phys Fluids* 2007;19:017107.
- [40] Dentz M, Bolster D, Le Borgne T. Concentration statistics for transport in random media. *Phys Rev E* 2009;80(11):010101.
- [41] Dentz M, Le Borgne T, Englert A, Bijeljic B. Mixing, spreading and reaction in heterogeneous media: a brief review. *J Contam Hydrol* 2011;120–121:1–17.
- [42] Ding D, Benson DA, Paster A, Bolster D. Modeling bimolecular reactions and transport in porous media via particle tracking. *Adv Water Resour* 2013;53:56–65. <http://dx.doi.org/10.1016/j.advwatres.2012.11.001>.
- [43] Donado LD, Sanchez-Vila X, Dentz M, Carrera J, Bolster D. Multicomponent reactive transport in multicontinuum media. *Water Resour Res* 2009;45(11).
- [44] Ebach EA, White RR. Mixing of fluids flowing through beds of packed solids. *AIChE J* 1958;4(2):161–9.
- [45] Edwards D, Brenner H. Macrotransport processes. Boston, Mass: Butterworth-Heinemann; 1993.
- [46] Engdahl NB, Ginn TR, Fogg GE. Scalar dissipation rates in non-conservative transport systems. *J Contam Hydrol* 2013;149:46–60.
- [47] Fernández-García D, Sánchez-Vila X. Optimal reconstruction of concentrations, gradients and reaction rates from particle distributions. *J Contam Hydrol* 2011;120:99–114.
- [48] Fernández-García D, Sánchez-Vila X, Guadagnini A. Reaction rates and effective parameters in stratified aquifers. *Adv. Water Res.* 2008;31(10):1364–76.
- [49] Fetter CW. Applied hydrogeology. 4th ed. Prentice Hall; 2001.
- [50] Gelhar LW, Axness CL. Three-dimensional stochastic analysis of macrodispersion in aquifers. *Water Resour Res* 1983;19(1):161–80.
- [51] Ginn TR, Simmons CS, Wood BD. Stochastic-convective transport with nonlinear reaction: biodegradation with microbial growth. *WRR* 1995;31:2689–700.
- [52] Goodrich MT, McCord JT. Quantification of uncertainty in exposure assessments at hazardous waste sites. *Ground Water* 1995;33:727–32.
- [53] Gramling CM, Harvey CF, Meigs LC. Reactive transport in porous media: a comparison of model prediction with laboratory visualization. *Environ Sci Technol* 2002;36:2508–14.

- [54] Hazen A. Some physical properties of sands and gravels, with special reference to their use in filtration. In: 24th Annual rep., Massachusetts State Board of Health, Pub. Doc. No. 34, 1892. p. 539–556.
- [55] Hazen A. Discussion of dams on sand foundations by A.C. Koenig. *Trans Am Soc Civ Eng* 1911;73:199–203.
- [56] Hassanizadeh SM, Leijnse A. A non-linear theory of high-concentration-gradient dispersion in porous media. *Adv Water Resour Res* 1995;18:203–15.
- [57] Hornung U. *Homogenization and porous media*. Springer; 1997.
- [58] Hoteit H, Mose R, Younes A, Lehmann F, Ackerer P. Three dimensional modeling of mass transfer in porous media using the mixed hybrid finite elements and random walk methods. *Math Geol* 2002;34:435–56.
- [59] Kapoor C, Gelhar LW. Transport in three-dimensionally heterogeneous aquifers 1. Dynamics of concentration fluctuations. *Water Resour Res* 1994;30(6):1775–88.
- [60] Kapoor V, Kitanidis PK. Concentration fluctuations and dilution in aquifers. *Water Resour Res* 1998;34(5):1181–93.
- [61] Kembrowski MW, Chang C-M, Kamil I. A mean behavior model of aerobic biodegradation in heterogeneous formation. *SHH* 1997;11:255–66.
- [62] Kinzelbach W. Simulation of pollutant transport in groundwater with the random walk method. *IAHS Publ* 1990;173:265–79.
- [63] Kitanidis PK. The concept of the dilution index. *Water Resour Res* 1994;30:2011–26.
- [64] Knutson C, Werth CJ, Valocchi AJ. Pore scale simulation of biomass growth along the transverse mixing zone of a model 2D porous medium. *Water Resour Res* 2005;41(7):W07007.
- [65] LaBolle EM, Fogg GE, Tompson AFB. Random-walk simulation of transport in heterogeneous porous media: local mass-conservation problem and implementation methods. *Water Resour Res* 1996;32(3):583–93.
- [66] LaBolle EM, Quastel J, Fogg GE, Gravner J. Diffusion processes in composite porous media and their numerical integration by random walks: generalized stochastic differential equations with discontinuous coefficients. *Water Resour Res* 2000;36(3):651.
- [67] LaBolle EM, Zhang Y. Reply to comment by D.-H. Lim on Diffusion processes in composite porous media and their numerical integration by random walks: Generalized stochastic differential equations with discontinuous coefficients'. *Water Resour Res* 2006;42:W02602.
- [68] Le Borgne T, Dentz M, Carrera J. Lagrangian statistical model for transport in highly heterogeneous velocity fields. *Phys Rev Lett* 2008;101(9):090601.
- [69] Le Borgne T, Dentz M, Carrera J. Spatial Markov processes for modeling Lagrangian particle dynamics in heterogeneous porous media. *Phys Rev E* 2008;78(2):026308.
- [70] Le Borgne T, Dentz M, Bolster D, Carrera J, de Dreuzy J, Davy P. Non-Fickian mixing: temporal evolution of the scalar dissipation rate in heterogeneous porous media. *Adv Water Resour* 2010;33:1468–75.
- [71] Le Borgne T, Dentz M, Davy P, Bolster D, Carrera J, De Dreuzy JR, Bour O. Persistence of incomplete mixing: a key to anomalous transport. *Phys Rev E* 2011;84(1):015301.
- [72] Lim D-H. Comment on Diffusion processes in composite porous media and their numerical integration by random walks: generalized stochastic differential equations with discontinuous coefficients by E.M. LaBolle, J. Quastel, G.E. Fogg, and J. Gravner. *Water Resour Res* 2006;42:W02601.
- [73] Luo J, Cirpka OA. How well do mean breakthrough curves predict mixing-controlled reactive transport? *Water Resour Res* 2011;47:W02520.
- [74] MacQuarrie KTB, Sudicky EA. Simulation of biodegradable organic contaminants in groundwater, 2, plume behavior in uniform and random flow fields. *WRR* 1990;26:223–39.
- [75] Mays DC, Neupauer RM. Plume spreading in groundwater by stretching and folding. *Water Resour Res* 2012;48:W07501.
- [76] Meerschaert MM, Zhang Y, Baeumer B. Tempered anomalous diffusion in heterogeneous systems. *Geophys Res Lett* 2008;35(17):L17403.
- [77] Molz FJ, Widdowson MA. Internal inconsistencies in dispersion-dominated models that incorporate chemical and microbial kinetics. *WRR* 1988;24:615–9.
- [78] Nambi IM, Werth CJ, Sanford RA, Valocchi AJ. Pore-scale analysis of anaerobic halo-respiring bacterial growth along the transverse mixing zone of an etched silicon pore network. *Environ Sci Tech* 2003;37(24):5617–24.
- [79] Neuman SP, Tartakovsky DM. Perspective on theories of non-Fickian transport in heterogeneous media. *Adv Water Resour* 2009;32(5):670–80.
- [80] Paster A. Mixing between fresh and salt waters at aquifer regional scale and identification of transverse dispersivity. *J Hydrol* 2010;380(36–44):2010.
- [81] Perkins TK, Johnston OC. A review of diffusion and dispersion in porous media. *Soc Petrol Eng J* 1963;3:70–84.
- [82] Pope SB. *Turbulent flows*. Cambridge University Press; 2000.
- [83] Pozrikidis C. *Numerical computation in science and engineering*. Oxford University Press; 1998.
- [84] Rahman MA, Jose SC, Nowak W, Cirpka OA. Experiments on vertical transverse mixing in a large-scale heterogeneous model aquifer. *J Contam Hydrol* 2005;80(3–4):130–48.
- [85] Raje DS, Kapoor V. Experimental study of bimolecular reaction kinetics in porous media. *Environ Sci Technol* 2000;34:1234–9.
- [86] Rolle M, Eberhardt C, Chiogna G, Cirpka OA, Grathwohl P. Enhancement of dilution and transverse reactive mixing in porous media: experiments and model-based interpretation. *J Contam Hydrol* 2009;10(3–4):130–42.
- [87] Singhal BBS, Gupta RP. *Applied hydrogeology of fractured rocks*. Springer Science and Business Media B.V; 2010.
- [88] Sternberg SPK. Dispersion measurements in highly heterogeneous laboratory scale porous media. *Transp Porous Media* 2004;54:107–24.
- [89] Sudicky EA, Schellenberg SL, MacQuarrie KTB. Assessment of the behavior of conservative and biodegradable solutes in heterogeneous porous media. In: Cushman JH, editor. *Dynamics of fluids in hierarchical porous media*. San Diego, Calif.: Academic; 1990. p. 429–62.
- [90] Takeda H, Farsiu S, Milanfar P. Kernel regression for image processing and reconstruction. *IEEE Trans Image Process* 2007;16(20):349–66.
- [91] Tartakovsky AM, Redden G, Lichtner P, Scheibe T, Meakin P. Mixing-induced precipitation: experimental study and multiscale numerical analysis. *Water Resour Res* 2008;44:W06S04.
- [92] Tartakovsky AM, Anna P, Le Borgne T, Balter A, Bolster D. Effect of spatial concentration fluctuations on effective kinetics in diffusion-reaction systems. *Water Resour Res* 2012;48(2).
- [93] Werth CJ, Cirpka OA, Grathwohl P. Enhanced mixing and reaction through flow focusing in heterogeneous porous media. *Water Resour Res* 2006;42:W12414.
- [94] Werner AD, Bakker M, Post VE, Vandenbohede A, Lu C, Ataie-Ashtiani B, Barry DA. Seawater intrusion processes, investigation and management: recent advances and future challenges. *Adv Water Resour* 2013;51:3–26.
- [95] Whitaker S. *The method of volume averaging*. Springer; 1998.
- [96] Xu M, Eckstein Y. Statistical analysis of the relationships between dispersivity and other physical properties of porous media. *Hydrogeol J* 1997;5:4–20.